9th IEEE International Conference on Power Electronics, Drives & Energy Systems PEDES 2020

December 16th – 19th, 2020





Venue

Malaviya National Institute of Technology Jaipur
मालवीय राष्ट्रीय प्रौद्योगिकी संस्थान जयपुर

2020 IEEE International Conference on Power Electronics, Drives and Energy Systems (PEDES) | 978-1-7281-5672-9/20/$31.00 ©2020 IEEE | DOI: 10.1109/PEDES49360.2020.9379835

Technical Session 56:

Track: TT3: Renewable Energy and Smart Grids
Venue: Zoom Platform

S/N	Paper ID	Title	Authors
399	589	Mitigation of SSR in Series-Compensated DFIG-Based Wind Farms with STATCOMs using a Nonlinear Backstepping Control Scheme	Tushar Kanti Roy, Subarto Kumar Ghosh, Md Shamim Anower, Md Apel Mahmud, Rajesh Kumar and Akash Saxena
400	690	Nonlinear Partial Feedback Linearizing Output Feedback Control of Islanded DC Microgrids	Md Apel Mahmud, Tushar Kanti Roy, Rajesh Kumar and Amanullah M. T. Oo
401	288	Improving the Efficiency of the DAB Converter of an On-board EV Charger Using Different Modulation Techniques	Parth Nayak , Suman Manda, Yusuf Gupta, Anshuman Shuklayand and Suryanarayana Doolla
402	318	Solar Energy Forecasting Using Modified Polynomial Neural Network	N C Sahoo, Rajendra Narayan Senapati and Akshaya K Pati
403	527	Effect of FOIDN+TID Damping Controller based GCSC on Load Frequency Control	Sumana Das, Subir Datta and Lalit Chandra Saikia
404	617	Modeling and Control of a Solid State Transformer Interfaced Wind Energy System with a Permanent Magnet Synchronous Generator	M. K. K. Prince, M. T. Arif, A. Gargoom, S. Saha, A.M. T. Oo and M. E. Haque.
405	245	Decentralized Primary and Distributed Secondary Control for Current Sharing and Voltage Regulation inDC Microgrid Clusters with HESS	Satabdy Jena, Narayana Prasad Padhy and Josep M. Guerrero.
406	345	Model Predictive Control based Coordinated Voltage Control in Active Distribution Network utilizing OLTC and DSTATCOM	Arunima Dutta, Sanjib Ganguly and Chandan Kumar

2020 IEEE International Conference on Power Electronics, Drives and Energy Systems (PEDES) | 978-1-7281-5672-9/20/$31.00 ©2020 IEEE | DOI: 10.1109/PEDES49360.2020.9379685

Mitigation of SSR in Series-Compensated DFIG-Based Wind Farms with STATCOMs using a Nonlinear Backstepping Control Scheme

Tushar Kanti Roy
Department of ETE
RUET
Rajshahi, Bangladesh
tkroy@ete.ruet.ac.bd

Subarto Kumar Ghosh
Department of EEE
RUET
Rajshahi, Bangladesh
ghosh.sk@eee.ruet.ac.bd

Md Shamim Anower
Department of EEE
RUET
Rajshahi, Bangladesh
msanower@eee.ruet.ac.bd

Md Apel Mahmud
School of Engineering
Deakin University
Geelong, Australia
apel.mahmud@deakin.edu.au

Rajesh Kumar
Department of Electrical Engineering
MNIT
Jaipur, India
rkumar.ee@mnit.ac.in

Akash Saxena
Department of Electrical Engineering
SKIT
Jaipur, India
aakash.saxena@hotmail.com

***Abstract*—A nonlinear backstepping control scheme is proposed in this work for the voltage source converter (VSC) used with the static synchronous compensator (STATCOM) in a doubly fed induction generator (DFIG)-based series compensated wind farm in order to mitigate sub-synchronous resonance (SSR) and improve the transient stability. The proposed scheme will regulate the reactive power requirement either by absorbing or supplying through the STATCOM for alleviating the SSR. At the same time, the tracking of other properties representing the dynamics of the STATCOM will be ensured through the proposed controller. The control inputs for the proposed nonlinear STATCOM controller are derived in a way that these satisfy the Lyapunov stability theory and ensure the appropriate tracking of all dynamics associated with the STATCOM. Simulation studies are conducted to justify the theoretical aspects of the proposed control scheme by developing the series compensated and grid-connected DFIG-based wind farm with the STACOM using MATLAB/SIMULINK platform. The high compensation level is considered for evaluating the performance under the worst case operating condition and the performance is compared with a traditional but finely tuned proportional integral (PI) controller in terms of eliminating fluctuations due to the SSR in the output responses of the DFIG-based wind farm.**

***Index Terms*—SSR, DFIG-based wind farm, backstepping controller, voltage source converter, transient stability.**

I. Introduction

Climate changes and energy security are main concerns all over the world for which renewable energy sources (RESs) are considered as solutions and the investment on such sources are rapidly increasing [1]. Among different types of RESs (e.g., tidal, biogas, fuel cell, solar photovoltaic, and so on); the wind power generation system is considered as the most competitive and fastest growing one [2]. All these large-scale wind generators are usually located far away from load centers which necessitate the upgradation of the existing transmission and distribution (T&D) infrastructure or construction of new T&D infrastructure in order to transfer the power to the grid [3]. However, the upgradation or construction of T&D infrastructure for accommodating power generated from wind farms are expensive and such developments are also time consuming [4]. Therefore, it is crucial to identify some ways through which the existing T&D infrastructure can be utilized and the series capacitive compensation (SCC) scheme is a way which reduces the inductive component of the transmission line for enhancing the power transfer capability [5]. However, wind farms including DFIG-based wind farms experience severe oscillations in different responses (e.g., voltage and power at different points) when the SCC scheme is employed. These oscillations appear due to the sub-synchronous resonance (SSR) which results from the interaction of impedances between the DFIG and rest of the power network even if the compensation level is quite low [6].

There are different approaches in the existing literature for mitigating oscillations due to the SSR. Among these, the simplest approaches are those which adjust impedances for power networks for eliminating the effects of the SSR [7]. However, the key limitation of these approaches is the efficiency and flexibility of power transmission capability as these are developed without capturing appropriate dynamics of series-compensated DFIG-based wind farms. For improving the efficiency and flexibility of the power transmission capability of series-compensated DFIG-based wind farms, the internal control structures of the GSC and RSC are modified in [8] using a SSR damping controller (SRDC). However, the performance of such modified internal control structures depends on the control schemes which are mostly linear in the existing literature though there are few nonlinear control schemes, e.g., partial feedback linearization in [9]. Another alternative way for effectively eliminating the impacts of

978-1-7281-5672-9/20/$31.00 ©2020 IEEE

the SSR is the installation of flexible AC transmission system (FACTS) devices that include static volt-ampere reactive compensators, thyristor-controlled series capacitors, static synchronous compensators (STATCOMs), etc. [10]. STATCOMs are considered as the mostly used among different FACTS devices as these provide appropriate reactive power support to the system for ensuring fast transient and steady-state voltage control at the point of common coupling (PCC). Hence, this work considers STATCOMs for mitigating the SSR in a series compensated DFIG-based wind farm so that the power transmission capability and transient stability are improved.

STATCOMs need to be controlled in a way that the effects of the SSR are eliminated and there are different control schemes which are designed by capturing the dynamics of STATCOMs [1], [6]. These controllers work perfectly for eliminating the SSR and improving the transient stability of the series compensated DFIG-based wind farms for a specific set of equilibrium points as these are designed by simplifying nonlinear dynamics of STATCOMs as linear. However, there are extremely high nonlinearities in DFIG-based wind farms where these nonlinearities originate from continuously varying wind speed for which the switching signals of voltage source converters (VSCs) within STATCOMs needs to be continuously adjusted which are quite impossible with linear control schemes. Furthermore, the dynamic characteristics of such DFIG-based wind farms significantly change when there are faults on the system, especially on grid sides where these wind generators supply power [11]. Hence, the controller for STATCOMs should be designed in such a way that it has the ability to mitigate the effects of the SSR under such conditions. A nonlinear partial feedback linearizing control scheme is proposed in [9] for the GSC and RSC to mitigate the SSR for series compensated DFIG-based wind farms. However, the controller is not designed for any external device, e.g., STATCOMs. Furthermore, the partial feedback linearizing scheme does not guarantee the stability of all states within the system and it is highly sensitive to parameter variations. A nonlinear sliding mode control (SMC) scheme is proposed in [12] for a partial feedback linearized series compensated DFIG-based wind farms to overcome the parameters sensitivity problems in [9] as it includes inherent properties to provide robustness against parameter variations. However, the control scheme in [12] is designed for the GSC and RSC while it still cannot guarantee the convergence of all properties of the system. The nonlinear backstepping control scheme has the feature to ensure the stability of all dynamics of a system for which it is designed [13]. However, to the best of authors knowledge, it has not been used for mitigating the SSR of series compensated DFIG-based wind farms either modifying internal control structures or controlling external FACTS devices.

The paper considers to design a nonlinear STATCOM controller to mitigate the SSR in a grid-connected DFIG-based wind farm in which the transmission line is compensated using a series capacitor. The nonlinear STATCOM controller is designed in this work using the backstepping control scheme which ensures the stability of all dynamics representing the actual behaviors of STATCOMs. The proposed controller will allow STATCOMs to release or absorb desired reactive power to ensure the desired performance for their dynamic properties and hence, the oscillations due to the SSR will be effectively eliminated. A systematic step by step approach will be followed to derive control signals for STATCOMs while analyzing their stability using the Lyapunov stability theory. Simulation studies are carried out by considering the high compensation level to demonstrate the applicability of the controller under worst case operating conditions and compared with a traditional proportional integral (PI) controller for demonstrating the superiority of the designed control scheme.

II. Dynamical Model of the System

Fig. 1 shows the schematic diagram of a series-compensated DFIG-based wind farm with a STATCOM where the rotor of the DFIG is connected with a back-to-back converter, i.e., rotor-side converter (RSC) and grid-side converter (GSC) while the stator is interfaced with the main grid. In this figure, the STATCOM is connected to the transmission line using a filter and transformer and the proposed nonlinear control scheme is employed on the STATCOM. The dynamical models of all components in Fig. 1, i.e., RSC, GSC, series-compensated transmission line, and STATCOM are discussed in the following subsections in order to provide an idea about the dynamic characteristics of these components though the controller will be designed only for the STATCOM.

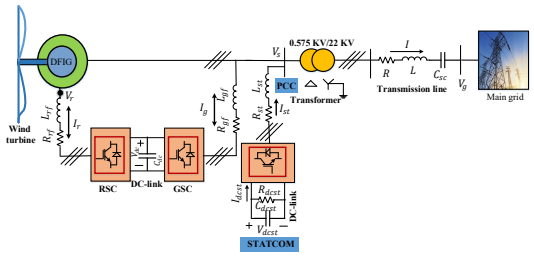

Fig. 1: Schematic diagram of a series-compensated DFIG wind farm along with a STATCOM connected to grid

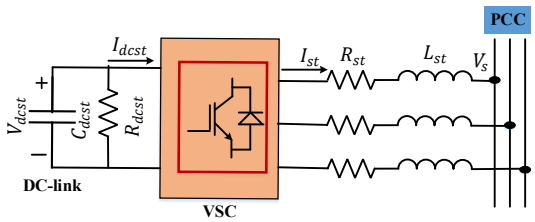

Fig. 2: Equivalent circuit diagram of a STATCOM as reactive power compensating device for a grid connected wind park system

A. Dynamics of the back-to-back converter (RSC and GSC)

The back-to-back converter in a DFIG-based wind farm works as a controlled voltage which is used to control the

978-1-7281-5672-9/20/$31.00 ©2020 IEEE

output current in straightforward way. For regulating the output current at the output of the RSC and GSC, it is essential to know the dynamic characteristics of these currents including the dynamic of the DC-link voltage bridging between the RSC and GSC.

*1) **RSC dynamics**:* The dynamics of the current at the output of the RSC can be expressed in the form of the following synchronously rotating dq reference frame [14]:

$$\begin{aligned}\dot{I}_{rd} &= -\frac{R_{rf}}{L_{rf}}I_{rd} - \omega_s I_{rq} - \frac{V_{dc}}{L_{rf}}S_{rd} + \frac{V_{rd}}{L_{rf}} \\ \dot{I}_{rq} &= -\frac{R_{rf}}{L_{rf}}I_{rq} + \omega_s I_{rd} - \frac{V_{dc}}{L_{rf}}S_{rq} + \frac{V_{rq}}{L_{rf}}\end{aligned} \tag{1}$$

*2) **GSC dynamics**:* The dynamics of the current at the output of the GSC can be represented as [14]:

$$\begin{aligned}\dot{I}_{gd} &= -\frac{R_{gf}}{L_{gf}}I_{gd} - \omega_s I_{gq} - \frac{V_{dc}}{L_{gf}}S_{gd} + \frac{V_{sd}}{L_{gf}} \\ \dot{I}_{gq} &= -\frac{R_{gf}}{L_{gf}}I_{gq} + \omega_s I_{gd} - \frac{V_{dc}}{L_{gf}}S_{gq} + \frac{V_{sq}}{L_{gf}}\end{aligned} \tag{2}$$

*3) **DC-link voltage dynamics**:* The dynamic of the voltage across the DC-link capacitor, linking the RSC and GSC, can be presented in terms of the following power balance equation:

$$C_{dc}V_{dc}\dot{V}_{dc} = P_r - P_g \tag{3}$$

with $P_r = \frac{3}{2}(V_{rd}I_{rd} + V_{rq}I_{rq})$ and $P_g = \frac{3}{2}(V_{ds}I_{gd} + V_{qs}I_{gq})$. The symbols as used in equations (1)-(3) represent their usual meanings whose definitions are provided in [14]. Since the transmission line is compensated with a series capacitance to enhance the power transmission capability, the dynamics of voltage and currents for such lines are presented in the following subsection.

B. Dynamics of series compensated transmission lines

The complete dynamics of any transmission line compensated by a series capacitor can be expressed in terms of the dynamics of the voltage across the capacitor and current flowing through the line. These dynamics can be expressed as [9]:

$$\begin{aligned}\dot{V}_{scd} &= \frac{1}{C_{sc}}I_d + \omega V_{scq} \\ \dot{V}_{scq} &= \frac{1}{C_{sc}}I_q - \omega V_{scd} \\ \dot{I}_d &= \frac{R}{L}I_d + \omega I_q + \frac{1}{L}(V_d - V_{scd} - E_d) \\ \dot{I}_q &= \frac{R}{L}I_q - \omega I_d + \frac{1}{L}(V_q - V_{scq} - E_q)\end{aligned} \tag{4}$$

where all these symbols carry the similar definitions as provided in [9]. Finally, it is essential to have the dynamics of the STATCOM as this is used to mitigate the SSR in series compensated DFIG-based wind farms and the dynamic model of a STATCOM is presented in the following subsection.

C. Dynamics of STATCOMs

STATCOMs are VSC-based shunt FACTS devices which are used in conjunction with series-compensated transmission lines through filters and transformers as is shown in Fig. 2. The key feature of a STATCOM is that it has the ability to absorb or deliver the reactive power, i.e., the bi-directional reactive power exchange capability between the PCC and its terminal. If the voltage at the PCC is lower than that of its desired value (which is also the terminal voltage of the STATCOM), the STATCOM will provide reactive power support to the PCC, i.e., act as a capacitor. Similarly, the STATCOM will absorb reactive power (i.e., act as an inductor) when the voltage at the PCC becomes higher than its desired value. This clearly indicates that the voltages at the PCC and the terminal of the STATCOM will be same under the normal operation and there will be no reactive power exchange. In this work, the SSR is mitigated by regulating the reactive power of the STATCOM so that the transient stability of the series-compensated DFIG-based wind farm can be improved. Since the controller will be designed by employing a nonlinear backstepping scheme, it is important to utilize a nonlinear dynamical model of the STATCOM and such a model can be developed in dq frame as discussed in [15] which can be written as:

$$\begin{aligned}\dot{V}_{dcst} &= \frac{1}{C_{dcst}}I_{dcst} - \frac{V_{dcst}}{R_{dcst}} \\ \dot{I}_{dst} &= -\frac{R_{st}}{L_{st}}I_{dst} + \omega I_{qst} + \frac{1}{L_{st}}(u_d V_{dcst} - V_{ds}) \\ \dot{I}_{qst} &= -\frac{R_{st}}{L_{st}}I_{qst} - \omega I_{dst} + \frac{1}{L_{st}}(u_q V_{dcst} - V_{qs})\end{aligned} \tag{5}$$

where V_{dcst} is the voltage across the DC-link capacitor; C_{dcst} is the DC-link capacitance; I_{dcst} is the input current of the VSC; R_{dcst} is the resistance of the converter representing conversion losses; I_{dst} and I_{qst} are d- and q-axis currents of the STATCOM, respectively; R_{st} and L_{st} are the equivalent resistance and reactance of the line connecting the STATCOM with the PCC, respectively; ω is the angular frequency; V_{ds} and V_{qs} are d- and q-axis voltages of the PCC, respectively; and u_d and u_q are control inputs in d- and q-axis, respectively. For the implementation, these control inputs need to be represented in terms of the modulation ratio (m) and firing angle (α) as expressed by following equations:

$$\begin{aligned}u_d &= m\sin\alpha \\ u_q &= m\cos\alpha\end{aligned} \tag{6}$$

Using equation (6), m and α can be calculated as:

$$\begin{aligned}m &= \sqrt{u_d^2 + u_q^2} \\ \alpha &= \tan^{-1}(\frac{u_d}{u_q})\end{aligned} \tag{7}$$

The static characteristics of the STATCOM can be represented the following equations of active power (P_{st}) and reactive power (Q_{st}):

$$\begin{aligned}P_{st} &= 1.5(V_{ds}I_{dst} + V_{qs}I_{qst}) \\ Q_{st} &= 1.5(V_{qs}I_{dst} - V_{ds}I_{qst})\end{aligned} \tag{8}$$

978-1-7281-5672-9/20/$31.00 ©2020 IEEE

For simplicity, it can be assumed that the average value of V_{qs} is zero at the steady-state. Under this assumption, equation (8) can be simplified as follows:

$$\begin{aligned} P_{st} &= 1.5 V_{ds} I_{dst} \\ Q_{st} &= -1.5 V_{ds} I_{qst} \end{aligned} \tag{9}$$

Now, the active power for the DC-side ($i.e., P_{dcst}$) of a STATCOM can be written as follows:

$$P_{dcst} = V_{dcst} I_{dcst} \tag{10}$$

Practically, the power loss due to R_{dcst} can be neglected as its value is always very small. Using this assumption, the active power at the DC- and AC-sides of the STATCOM will be equal to each other, i.e.,

$$P_{dcst} = P_{st} \tag{11}$$

Equation (5) can be simplified using equations (8)-(11) and finally, the dynamics of the STATCOM can be written as:

$$\dot{V}_{dcst} = \frac{1}{V_{dcst} C_{dcst}} 1.5 V_{ds} I_{dst} - \frac{V_{dcst}}{R_{dcst}} \tag{12}$$

$$\dot{I}_{dst} = -\frac{R_{st}}{L_{st}} I_{dst} + \omega I_{qst} + \frac{1}{L_{st}} u_d V_{dcst} - V_{ds} \tag{13}$$

$$\dot{I}_{qst} = -\frac{R_{st}}{L_{st}} I_{qst} - \omega I_{dst} + \frac{1}{L_{st}} u_q V_{dcst} \tag{14}$$

Based on this model as described by equations (12)-(14), the nonlinear backstepping controller will be designed in the following section.

III. Proposed Controller Design for STATCOMs

Since the reactive power exchange or regulation between the PCC and terminal of the STATCOM will ensure the desired voltage at the PCC while eliminating the effects of the SSR, this is main control objective for the proposed STATCOM controller. This control objective can easily be achieved with proposed backstepping control scheme by controlling I_{qst} in equation (9) towards its corresponding desired value. Furthermore, the proposed scheme ensures the convergence other physical properties represented though states in equations (12)-(14). The detailed and step-by-step process to design the proposed backstepping controller for the STATCOM are shown in the following.

Step 1: By following the sequence of states in equations (12)-(14), the first control objective is chosen to ensure the desired value $V_{dcst(ref)}$ of the DC-link voltage of the STATCOM for which the tracking error (e_1) will be as follows:

$$e_1 = V_{dcst} - V_{dcst(ref)} \tag{15}$$

and its dynamic after substituting equation (12) can be written as follows:

$$\dot{e}_1 = \frac{1.5}{V_{dcst} C_{dcst}} V_{ds} I_{dst} - \frac{V_{dcst}}{R_{dcst}} - \dot{V}_{dcst(ref)} \tag{16}$$

At this stage, the objective is to make $e_1 \rightarrow 0$ which is possible if $V_{dcst} \approx V_{dcst(ref)}$. In order to analyze this, a control Lyapunov function (CLF) is defined as follows:

$$W_1 = \frac{1}{2} e_1^2 \tag{17}$$

According to the Lyapunov stability theory, $e_1 \rightarrow 0$, i.e., $V_{dcst} \approx V_{dcst(ref)}$ when $\dot{W}_1$ becomes negative definite ($\dot{W}_1 < 0$) or semi-definite ($\dot{W}_1 \leq 0$). Thus, $\dot{W}_1$ using the value of $\dot{e}_1$ can be simplified as:

$$\dot{W}_1 = e_1 [\frac{1.5}{V_{dcst} C_{dcst}} V_{ds} I_{dst} - \frac{V_{dcst}}{R_{dcst}} - \dot{V}_{dcst(ref)}] \tag{18}$$

Since the actual control inputs do not appear in equation (18), a virtual control input (α) needs to be considered (as per the proposed backstepping scheme) where α corresponds to the next state in equations (12)-(14) which is I_{dst}, i.e., $\alpha \approx I_{dst}$ for stabilizing $\dot{e}_1$. Equation (18) will be semi-definite if the following condition holds:

$$\frac{1.5}{V_{dcst} C_{dcst}} V_{ds} \alpha - \frac{V_{dcst}}{R_{dcst}} - \dot{V}_{dcst(ref)} = -k_1 e_1 \tag{19}$$

with $k_1 > 0$ as a parameter controlling the convergence speed of e_1. From (19), α can be determined as:

$$\alpha = \frac{V_{dcst} C_{dcst}}{1.5 V_{ds}} (\frac{V_{dcst}}{R_{dcst}} + \dot{V}_{dcst(ref)} - k_1 e_1) \tag{20}$$

Substituting equation (19) into equation (20), $\dot{W}_1$ will be as follows:

$$\dot{W}_1 = -k_1 e_1^2 \tag{21}$$

which clearly indicates $\dot{W}_1 \leq 0$ for any value of e_1. At this point, it is essential to proceed to the next step where the actual control inputs will appear.

Step 2: Since $\alpha \approx I_{dst}$, the control action should minimize the error (e_2) between α and I_{dst}. Hence, e_2 can be defined as:

$$e_2 = I_{dst} - \alpha \tag{22}$$

and its dynamic after substituting equation (13) can be written as:

$$\dot{e}_2 = -\frac{R_{st}}{L_{st}} I_{dst} + \omega I_{qst} + \frac{1}{L_{st}} (u_d V_{dcst} - V_{ds}) - \dot{\alpha} \tag{23}$$

As u_d appears in (23), the error e_3 corresponding to I_{qst} can be analyzed in this step and the convergence of both I_{dst} and I_{qst} can also be analyzed together. If $I_{qst(ref)}$ represents the desired value of I_{qst}, e_3 can be written as:

$$e_3 = I_{qst} - I_{qst(ref)} \tag{24}$$

and its dynamic after substituting equation (14) can be written as follows:

$$\dot{e}_3 = -\frac{R_{st}}{L_{st}} I_{qst} - \omega I_{dst} + \frac{1}{L_{st}} u_q V_{dcst} - \dot{I}_{qst(ref)} \tag{25}$$

From equation (25), it is obvious that it includes u_q. Now, the main task is to determine u_d and u_q for which dynamics of the STATCOM become stable. This can be done by formulating the CLF as:

$$W_2 = W_1 + \frac{1}{2} (e_2^2 + e_3^2) \tag{26}$$

978-1-7281-5672-9/20/$31.00 ©2020 IEEE

whose derivative will be:

$$\dot{W}_2 = -k_1 e_1^2 + e_2[\frac{-R_{st}}{L_{st}} I_{dst} + \omega I_{qst} + \frac{1}{L_{st}}(u_d V_{dcst} - V_{ds}) - \dot{\alpha}] + e_3[\frac{-R_{st}}{L_{st}} I_{qst} - \omega I_{dst} + \frac{1}{L_{st}} u_q V_{dcst} - \dot{I}_{qst(ref)}] \quad (27)$$

At this stage, u_d and u_q will stabilize the dynamics of the STATCOM if the following conditions hold:

$$\begin{aligned} -\frac{R_{st}}{L_{st}} I_{dst} + \omega I_{qst} + \frac{1}{L_{st}}(u_d V_{dcst} - V_{ds}) - \dot{\alpha} &= -k_2 e_2 \\ -\frac{R_{st}}{L_{st}} I_{qst} - \omega I_{dst} + \frac{1}{L_{st}} u_q V_{dcst} - \dot{I}_{qst(ref)} &= -k_3 e_3 \end{aligned} \quad (28)$$

as these will make $\dot{W}_2 < 0$ or $\dot{W}_2 \leq 0$. Here, $k_1 > 0$ and $k_2 > 0$ are parameters used to control the convergence speed of e_2 and e_3, respectively. From equation (28), u_d and u_q can be calculated as:

$$u_d = \frac{L_{st}}{V_{dcst}}(\frac{R_{st}}{L_{st}} I_{dst} - \omega I_{qst} + \frac{1}{L_{st}} V_{ds} + \dot{\alpha} - k_2 e_2) \quad (29)$$

$$u_q = \frac{L_{st}}{V_{dcst}}(\frac{R_{st}}{L_{st}} I_{qst} + \omega I_{dst} + \dot{I}_{qst(ref)} - k_3 e_3) \quad (30)$$

With these control laws, equation (28) can be represented as:

$$\dot{W}_2 = -k_1 e_1^2 - k_2 e_2^2 - k_3 e_3^2 \quad (31)$$

Equation (31) clearly shows that $\dot{W}_2 \leq 0$ for any value of the errors. The following section discusses the improvement in the SSR with the designed nonlinear STATCOM controller.

IV. Simulation Results

The designed nonlinear STATCOM controller is implemented on a series compensated grid-connected DFIG-based wind farm with a STATCOM as shown Fig. 1. In this wind farm, six DFIG-based wind generators are connected to a PCC where the PCC voltage is 575 V and the power capacity of each wind generator 1.5 MW which makes the total capacity as 9 MW. A step up transformer is used in this wind farm for stepping up the voltage form 575 V to 25 kV and then connected with the main grid. For compensating the inductive element of the transmission with an aim of improving the power transfer capability, a capacitor 100 μF is placed in series at the middle of a 25 km transmission line (Z=0.1153+j0.3958 Ω/km). The STATCOM is connected at the grid, i.e., the high voltage side of the step-up transformer. In this work, the desired value of the DC-link voltage for the STATCOM is set as 1150 V while the value of this capacitor as 0.1 F and the switching frequency for VSC as 5 kHz. The system model in Fig. 1 is developed in MATLAB/SIMULINK platform. It is worth stressing that the backstepping scheme is only used for the STATCOM while other converters (i.e., RSC and GSC) within the DFIG-based wind farm are controlled using PI controllers. For validating the performance of the designed nonlinear backstepping STATCOM controller (BSSC), the worst case scenario, i.e., the higher value of the compensation level is considered during the simulation. The reason behind this is that if the BSSC performs well in the worst case,

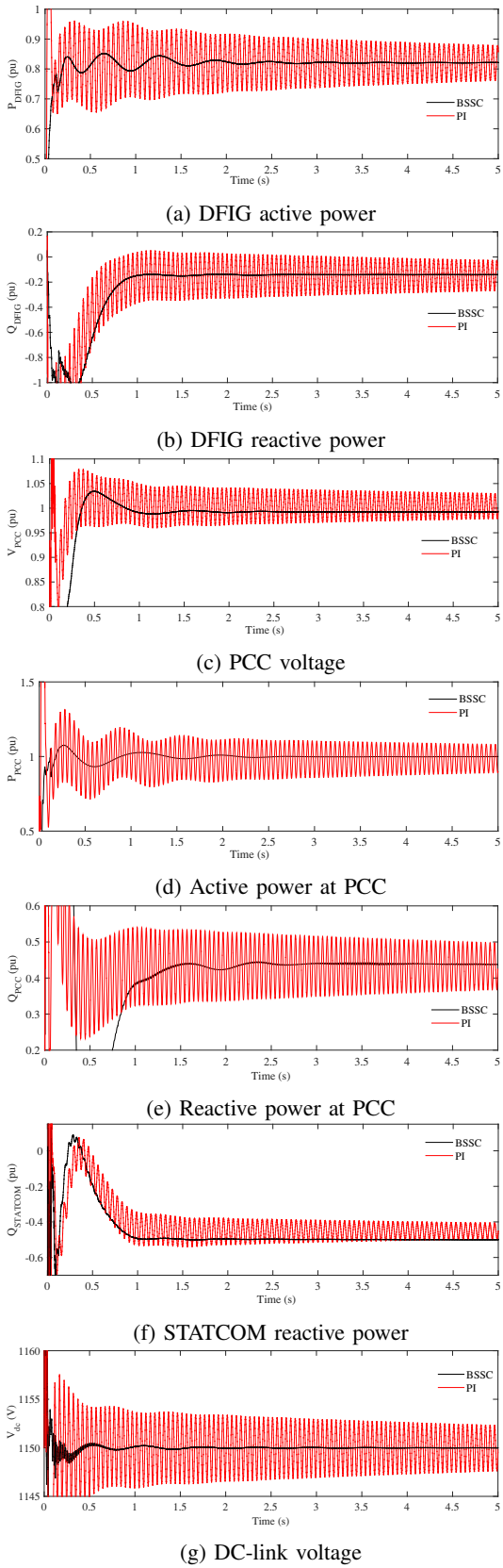

(a) DFIG active power

(b) DFIG reactive power

(c) PCC voltage

(d) Active power at PCC

(e) Reactive power at PCC

(f) STATCOM reactive power

(g) DC-link voltage

Fig. 3: Different physical properties of DFIG-based wind farm for a compensation level of 80% while having the wind speed as 8 m/s

978-1-7281-5672-9/20/$31.00 ©2020 IEEE

it will definitely work under other operating scenarios. The simulations are performed by considering 80% compensation level while considering the wind speed as the constant at 8 m/s. Finally, the performance of the designed BSSC is compared with a traditional PI controller.

The SSR is the results of interactions of impedances between a series compensated DFIG-based wind generator and the rest of the power network. Different important physical properties of a series-compensated DFIG-based wind farm with both BSSC and PI controllers for the STACOM are provided in Fig. 2. These properties include the active and reactive power of the DFIG; voltage, active, and reactive power at the PCC; reactive power of the STATCOM; and DC-link voltage for the STATCOM. The active and reactive power responses for the DFIG, as illustrated in Figs. 3 (a) and (b), respectively; show that there are oscillations in these responses when the PI controller is used. From these figures, it can also be observed that the magnitudes of these oscillations are reducing when the STATCOM is controlled by the PI controller. Hence, these oscillations persist for a while which will create transient stability issue for the whole wind farm. However, these are not the cases when the BSSC is used as the oscillations have quickly damped out which means that the transient stability is ensured within around 2 s. These effects will also be propagated on remaining parts of the system and these can be evidenced from relevant power (both active and reactive) and voltage (both PCC and DC-link) responses as shown in Figs. 3 (c) to (g).

From all these figures, it can be observed that the series compensated DFIG-based wind farm experiences SSR which introduces oscillating characteristics with decreasing amplitudes similar to that as discussed earlier on. In these figures, the oscillations last for a while if the PI controller is used for the STATCOM though these are very quickly eliminated with the BSSC. All these happen as the designed BSSC ensures the appropriate reactive power exchange between the terminal of the STATCOM and PCC. From simulation results in Fig. 3, it is evident that the designed BSSC effectively mitigates the effects of the SSR and helps system to preserve the transient stability for a highly compensated DFIG-based wind farm with a series compensator. The BSSC always performs better than the PI controller and thus, effectively transfer power through the transmission line.

V. Conclusion

A nonlinear backstepping control scheme is employed for STATCOMs in a series compensated DFIG-based wind farm with extremely high compensation level. Theoretically, the designed scheme shows that it guarantees the convergence of all state representing dynamics of STATCOMs while ensuring the stability. Simulation results clearly justify the theoretical findings and it can be clearly seen that the designed controller eliminates the SSR within the timeframe (around few seconds) for the transient stability whereas oscillations due to the SSR last for a while when the PI controller is used. The results clearly indicate that the transient stability of the series compensated DFIG-based wind farm with a STATCOM is effectively enhanced with the designed controller and hence, the power transfer capability is improved. However, the nonlinear backstepping scheme still requires the exact parameters of the system which can be overcome in a future work by employing an adapting backstepping scheme as it has the ability to adapt all parameters within STATCOMs.

References

[1] R. K. Varma, S. Auddy, and Y. Semsedini, "Mitigation of subsynchronous resonance in a series-compensated wind farm using FACTS controllers," *IEEE Transactions on Power Delivery*, vol. 23, no. 3, pp. 1645–1654, 2008.

[2] T. K. Roy, M. A. Mahmud, S. N. Islam, and A. M. T. Oo, "Nonlinear adaptive backstepping controller design for permanent magnet synchronous generator (PMSG)-based wind farms to enhance fault ride through capabilities," in *2019 IEEE Power Energy Society General Meeting (PESGM)*, 2019, pp. 1–5.

[3] F. Salehi, I. B. M. Matsuo, A. Brahman, M. A. Tabrizi, and W.-J. Lee, "Sub-synchronous control interaction detection: A real-time application," *IEEE Transactions on Power Delivery*, vol. 35, no. 1, pp. 106–116, 2019.

[4] D. Suriyaarachchi, U. Annakkage, C. Karawita, and D. Jacobson, "A procedure to study sub-synchronous interactions in wind integrated power systems," *IEEE Transactions on Power Systems*, vol. 28, no. 1, pp. 377–384, 2012.

[5] C. Karunanayake, J. Ravishankar, and Z. Y. Dong, "Nonlinear SSR damping controller for dfig based wind generators interfaced to series compensated transmission systems," *IEEE Transactions on Power Systems*, vol. 35, no. 2, pp. 1156–1165, 2019.

[6] G. Li, Y. Chen, A. Luo, and H. Wang, "An enhancing grid stiffness control strategy of STATCOM/BESS for damping sub-synchronous resonance in wind farm connected to weak grid," *IEEE Transactions on Industrial Informatics*, vol. 16, no. 9, pp. 5835–5845, 2019.

[7] Y. Meng, X. Pan, H. Ma, K. Li, J. Yu, and X. Wang, "Analysis and mitigation of subsynchronous resonance based on integral control for DFIG-based wind farm," *IET Generation, Transmission & Distribution*, vol. 13, no. 9, pp. 1718–1725, 2019.

[8] H. Mohammadpour and E. Santi, "Optimal adaptive sub-synchronous resonance damping controller for a series-compensated doubly-fed induction generator-based wind farm," *IET Renewable Power Generation*, vol. 9, no. 6, pp. 669–681, 2015.

[9] M. A. Chowdhury, M. A. Mahmud, W. Shen, and H. R. Pota, "Nonlinear controller design for series-compensated DFIG-based wind farms to mitigate subsynchronous control interaction," *IEEE Transactions on Energy Conversion*, vol. 32, no. 2, pp. 707–719, 2017.

[10] D. Shu, X. Xie, H. Rao, X. Gao, Q. Jiang, and Y. Huang, "Sub-and super-synchronous interactions between STATCOMs and weak AC/DC transmissions with series compensations," *IEEE Transactions on Power Electronics*, vol. 33, no. 9, pp. 7424–7437, 2017.

[11] T. K. Roy, M. A. Mahmud, S. N. Islam, K. M. Muttaqi, and A. M. T. Oo, "Nonlinear adaptive direct power controllers of DFIG-based wind farms for enhancing FRT capabilities," in *2019 IEEE Industry Applications Society Annual Meeting*, 2019, pp. 1–6.

[12] P. Li, J. Wang, L. Xiong, and M. Ma, "Robust nonlinear controller design for damping of sub-synchronous control interaction in DFIG-based wind farms," *IEEE Access*, vol. 7, pp. 16 626–16 637, 2019.

[13] T. K. Roy and M. A. Mahmud, "Dynamic stability analysis of hybrid islanded DC microgrids using a nonlinear backstepping approach," *IEEE Systems Journal*, vol. 12, no. 4, pp. 3120–3130, 2018.

[14] T. K. Roy, M. A. Mahmud, S. N. Islam, A. M. Oo, and K. Muttaqi, "Enhancement of fault ride through capabilities for grid-connected DFIG-based wind farms using nonlinear adaptive backstepping controllers," in *2018 IEEE International Conference on Power Electronics, Drives and Energy Systems (PEDES)*. IEEE, 2018, pp. 1–6.

[15] M. A. Mahmud, H. Pota, and M. Hossain, "Nonlinear DSTATCOM controller design for distribution network with distributed generation to enhance voltage stability," *International Journal of Electrical Power & Energy Systems*, vol. 53, pp. 974–979, 2013.

978-1-7281-5672-9/20/$31.00 ©2020 IEEE